ecoPETROL

ctyf@ecopetrol.com.co

EFFECT OF THE STRUCTURAL CHARACTERISTICS OF NAPHTHENIC ACIDS ON THE CORROSION KINETICS OF AN AISI SAE 1005

EFECTO DE LAS CARACTERÍSTICAS ESTRUCTURALES DE LOS ÁCIDOS NAFTÉNICOS EN LA CINÉTICA DE CORROSIÓN DE UN ACERO AISI SAE 1005

Carlos Mejía-Miranda[1]*, Haydee Becerra-Quiroga [2], Darío Peña-Ballesteros[1], Dionisio Laverde-Cataño [1], Helmuth Sarmiento-Klapper[3] .

ABSTRACT

Processing crudes with high naphthenic acid content causes corrosion problems on the crude oil distillation units. The total acid number (*TAN*) is commonly used to evaluate the corrosivity of crude oils; thus for decision-making related to corrosion mitigation and control in refineries. However, the *TAN* only represents the number of carboxylic groups present in the crude oil and does not consider the structural characteristics of the naphthenic acids, nor their reactivity, which are highly relevant to corrosion. On the other hand, the study of naphthenic acids as fractions with specific structural characteristics should enable the identification of differences in the corrosivity of crude oil with the same naphthenic acid concentration. In this research work, the fractioning of a commercial mixture of naphthenic acids was performed using the ionic strength of their respective salts. The structural characterization of the obtained fractions was conducted using Fourier-transform infrared and mass spectroscopy, gel permeation chromatography, and nuclear magnetic resonance. Furthermore, the corrosion rate of AISI SAE 1005 steel exposed to each fraction of naphthenic acids in the temperature range between 270 and 350 ºC was determined. Based on these results, a kinetic model of parallel reactions for predicting the concentration of dissolved iron in crude oil containing a mixture of naphthenic acids is proposed and validated.

RESUMEN

El procesamiento de crudos con alto contenido de ácidos nafténicos causa problemas de corrosión en las unidades de detilación. El Número Total Ácido (TAN) es comunmente usado para evaluar la corrosividad de crudos, y por lo tanto es un parametro usado para la toma de decisiones relacionadas con el control de la corrosión de la refinerias. Sin embargo, el *TAN* solo representa el número de grupos carboxílicos presentes en el crudo y no considera las características estructurales de los ácidos nafténicos ni su reactividad en las reacciones de corrosión. En este trabajo se desarrolló el fraccionamiento de una mezcla comercial de ácidos nafténicos a partir de la solubilidad de sus respectivas sales. Se determinaron parámetros estructurales característicos de los ácidos nafténicos de cada fracción usando Espectroscopia de Infrarrojo, Cromatografía De Permeación en Gel, Resonancia Magnética Nuclear, Espectroscopia de Masas y Análisis Elemental. Se realizó el estudio cinético de la reacción de corrosión de un acero AISI 1005 expuesto a cada fracción de ácidos nafténicos en el rango de temperatura entre 270 y 350°C. Finalmente, se propuso un modelo de reacciones paralelas para la predicción de la concentración de hierro disuelto debido a la reacción de corrosión, a partir de la concentración molar de cada una de las fracciones que conforman la mezcla de ácidos nafténicos.

KEYWORDS / PALABRAS CLAVE

Naphthenic acids | corrosion | crude oils | AISI SAE 1005
Ácidos Nafténicos | corrosión | refinación | AISI SAE 1005

AFFILIATION

[1] *Universidad Industrial de Santander, Colombia.*
[2] *Instituto Colombiano del Petróleo, ECOPETROL, Colombia*
[3] *Center for Materials Research, Baker Hughes, Celle, Germany*
email:caumejia@gmail.com

1. INTRODUCTION

The significant reduction of conventional oil resources has led the oil and gas industry to increase considerably the percentage of non-conventional oil in blends entering the crude oil distillation units. [1] High acid-containing crudes are commonly found in the so-called non-conventional or opportunity crude oils. Due to their low quality, characterized typically by a significant content of contaminants including corrosive naphthenic acids and sulfur-bearing compounds, opportunity crude oils are considerably less expensive and more readily available in the oil market as compared to conventional crude. However, processing opportunity crude oils forces the refineries to establish special strategies for mitigating their corrosive effects on the distillation units.. Corrosion due to naphthenic acids and sulfur present in opportunity crude oils occurs in the temperature range of 220 to 400 °C, primarily in the transfer lines of distillation units. [2,3] The general reaction that describes naphthenic acid corrosion is shown in Equation 1. [3,4,5]

$$2RCOOH + Fe \rightarrow Fe(RCOO)_2 + H_2 \qquad (1)$$
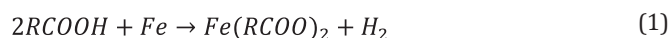
The total acid number (*TAN*) of a crude oil is associated mainly with its content of naphthenic acids, which are formed by biodegradation processes. [6] The *TAN* is defined as the milligrams of KOH required to neutralize one gram of crude oil. [7-9] It is typically used in refineries to define blends that enter the distillation units r to establish the appropriate corrosion control strategy. However, practical experience has demonstrated that crude oils having the same total concentration of naphthenic acids and sulfur compounds can have different corrosivity. [10-11] In addition, experimental results have demonstrated that the corrosivity of crude oil relates not only to the total concentration of naphthenic acids, but also to the chemical nature of these compounds. [2,3,10-12,] Therefore, the heterogeneity of these species does not allow to establish a prediction strategy purely based on *TAN* to meet industry requirements. The aim of this research work was to study the variation in the reactivity of single fractions of naphthenic acids for better understanding the corrosivity of a mixture of them on carbon steel AISI SAE 1005, based on the proportion of these fractions in one commercial blend.

2. EXPERIMENTAL SECTION

MATERIALS

Rectangular carbon steel AISI SAE 1005 coupons which dimensions are 30.65 mm , by 17.85 mm width, and 2.93 mm in thickness were used for exposure tests according to ASTM G-31. [13] The chemical composition of the carbon steel studies, which is commonly used in refinery equipment, was established by optical emission spectroscopy (OES). The investigated material contains 0.055 wt.% C, 0.172 wt.% Mn, 0.0087 wt.% P, 0.047 wt.% Al, and 0.025 wt% Cr. In addition, a commercial naphthenic acid blend of crude oil was used.

FRACTIONING OF NAPHTHENIC ACIDS

A sample of 15 g from the blend was dissolved in 200 ml of dichloromethane (DCM) and washed three times with 100 ml of a 1M NaOH solution prepared with a 1:1 EtOH/H2O mixture as solvent. The insoluble fraction in the aqueous solution (Fraction 1) was separated by decanting and subsequent evaporation of the DCM. The alkali aqueous phase was gradually acidified by the addition of a concentrated HCl solution, obtaining two additional fractions: Fraction 2 corresponds to the insoluble naphthenic acids at pH 7, and Fraction 3 corresponds to the fraction of insoluble naphthenic acids at pH 1. Fraction 4 corresponds to the total extractable fraction (Fractions 2 and 3). This procedure was performed often to obtain a sufficient amount of each fraction of naphthenic acids for the required tests. The mole percent of each fraction in the commercial blend was determined using Equation 2, where, $\% M_i$ is the mole percent of each fraction extracted, W_{NAi} (g) is the weight of each fraction., TAN_i (mgKOH/g) is the total acid number of each fraction and $W(g)$ is the initial weight of the commercial blend, 230 is the *TAN* of the commercial mixture of naphthenic acids. The *TAN* was determined according to ASTM D664.[14]

$$\%M_i = \frac{W_{NAi} * TAN_I}{W * 230} * 100 \qquad (2)$$

CHARACTERIZATION OF NAPHTHENIC ACIDS FRACTIONS

The fractions were characterized by elemental analysis, Fourier-transform infrared spectroscopy (FTIR), Gel Permeation Chromatography (GPC), Nuclear Magnetic Resonance (NMR), and Mass Spectroscopy (MS).

ACQUISITION OF FTIR-SPECTRA
FTIR experiments were performed using a SHIMADZU 8400S FTIR instrument. All spectra were obtained in the absorbance mode with a scan range of 4000-450 cm-1 and a resolution of 4 cm-1 for 10 scans. The samples were prepared by dissolving 6-8 mg of the fraction in 4 mL of DCM. A drop of the sample was placed on the sample holder and the DCM was allowed to evaporate.

ELEMENTAL CHARACTERIZATION
Analytical determination of C, H, N, S was performed by a Thermo ScientificTM analyzer.

1H NMR AND 13C NMR MEASUREMENTS
The 1H NMR and 13C NMR spectra of the fraction were obtained using a Bruker Avance III 400 MHz spectrometer in 5 wt.% solutions of CDCl3 containing tetramethylsilane (TMS) as internal reference. Pulses of 30° (Bruker zg30 pulse sequence) with pre-scan delay of 10.0 μs were used, and the delay time between the scans was 10 s. The sweep width was 6000 Hz, and the acquisition time was 5.45 s. In total, 32 scans were averaged for each spectrum and used for the statistical analysis. The phase and baseline of the resulting spectra were manually adjusted and corrected after using a very large expansion of the y-axis. The integration was performed within each of these spectral segments, minimizing the small shifts observed from sample to sample. This was achieved by carefully setting the TMS signal to 0 ppm and normalizing the resulting integrals of the different segments of the spectrum.

GEL PERMEATION CHROMATOGRAPHY (GPC)

The molecular distribution was determined by GPC using a Waters 2414 refractive index detector at a column temperature of 40°C, using mobile phase and Tetrahydrofuran (THF). The average molecular weight (M_w) was calculated using Equation 3, where M_i and I_i correspond to the molecular weight and intensity of each acid in the blend, respectively.

$$Mw = \sum I_i M_i^2 / \sum I_i M_i \qquad (3)$$

MASS SPECTROMETRY

MS and MS/MS experiments were performed using a Thermo Finnigan Mass Spectrometer controlled by Tuneplus software (Excalibur), with the Electrospray Ionization (ESI) source in negative ion mode. The concentration of the sample consisted in 1-2 mg of the fraction dissolved in 2 ml of solvent; which was toluene. The sample flow rate was 4-6 μL/min and the mass scan range was between 180-2000 m/z. The mass spectra were based on 3 micro-scans with a 50 ms ion injection time, and automatic gain control was enabled. The sheath gas was maintained at 60 psi, the temperature of the API stack at 220 °C, the capillary voltage was set at 7 V, and the spray voltage at 3.15 kV. Again, Equation 3 was used to calculate the average molecular weight.

CORROSION KINETIC STUDY

The experimental conditions for the corrosion tests are included in Table 1. The kinetic study was performed in a reactor manufactured using Hastelloy® C-276 (UNS N10276), with capacity for 50 mL.

Table 1. Experimental conditions for Corrosion Tests

Parameter	Conditions
Temperature (°C)	270, 290, 320 and 350
Time of reaction (h)	3, 6, 9 and 12

Each fraction of naphthenic acids was dissolved in white mineral oil. Before testing, all the surfaces of the coupon were prepared by mechanically grinding up to 1500 grit using SiC-paper. The dimension of the coupon was measured with a caliper and the coupon was then cleaned with deionized water, degreased in acetone, and dried in air. Finally, the coupon was weighted using an analytical scale (0.0001 g). All experimental conditions were tested in duplicate. After each test, the coupon was cleaned ultrasonically in acetone and weighted using the same analytical scale.

From the weight loss of the coupon, the number of moles of naphthenic acids consumed in the reaction was calculated. This has been called reactivity, and it is expressed in mg of iron (**Fe**) per kmol of naphthenic acids (**TAN**). Assuming a molar excess of iron in the reaction, the kinetic of reducing the acidity of crude due to the corrosion reaction can be represented by Equation 4, where **TAN** represents the total acid number in the white mineral oil, t represents the reaction time, k represents the reaction rate constant, and n represents the reaction order, which can be determined by experimental data.

$$-\frac{d\,TAN}{dt} = k * TAN^n \qquad (4)$$

Equation 4 considers that the change of acidity in the solution only relates to the reaction of naphthenic acids with the carbon steel. Assuming a first-order reaction:

$$-\frac{1}{TAN} d\,TAN = kdt \qquad (5)$$

Equation 6 results from solving the integral of equation 5, where TAN_i corresponds to the initial TAN.

$$ln\frac{TAN}{TAN_i} = kt \qquad (6)$$

In addition, the conversion reaction can be expressed as follows:

$$X = \frac{TAN}{TAN_i} \qquad (7)$$

Substituting equation 7 in Equation 6.

$$\ln X = kt \qquad (8)$$

Where k, for the first-order reaction, can be calculated from the slope of the linear plot of ln X vs. time.

Assuming a second-order reaction:

$$-\frac{d\,TAN}{dt} = k'TAN^2 \qquad (10)$$

Similar to Equation 7:

$$TAN = TAN_i X \qquad (11)$$

Substituting equation 11 in Equation 10:

$$-TAN_i \frac{d\,X}{dt} = k'(TAN_i X)^2 \qquad (12)$$

Solving the integral of Equation 12:

$$\frac{1}{X} - 1 = k'TAN_i t \qquad (13)$$

Thus, the reaction rate constant for the second-order reaction can be calculated from the slope of the linear plot of 1/X vs. time.

Statistical parameters such as percentages of Mean Square Error (*%RMSE*) and model efficiency (*EF*) were determined using Equations 14 to 16, [15,16] where y' is the value predicted by the model, yi is the measured value, m is the number of measurements, and Yi' is the mean of the measured values.

$$RMSE = \sqrt{\sum_{I=1}^{m} \frac{(yi-y')^2}{m}} \qquad (14)$$

$$\%RMSE = \left[\frac{RMSE}{Yi'}\right].100 \qquad (15)$$

$$EF = 1 - \frac{\sum_{i=1}^{m}(y\prime-yi)^2}{\sum_{i=1}^{m}(yi-Yi\prime)^2} \qquad (16)$$

In general, the accuracy of a model is considered excellent when *%RMSE* < 10%, good if 10 ≤ *%RMSE* < 20, acceptable when 20 < *%RMSE* ≤ 30, and not so exact when the *%RMSE* exceeds 30%. Similarly, a model is considered efficient if *EF* ≥ 0.6.

3. RESULTS AND DISCUSSION

FRACTIONATION OF NAPHTHENIC ACIDS

The molar percent of each of the fractions of naphthenic acids is shown in Figure 1. Fraction 1 has *TAN* = 0; therefore, the total number of moles of carboxylic groups is distributed in fractions 2 and 3, indicating that fraction 1 does not contribute to the acidity of the commercial mixture of naphthenic acids. The weight percentage of fraction 1 in the commercial blend of naphthenic acids was 22.94%. Other researchers have reported that this fraction corresponds to a mixture of esters, hydrocarbons, and benzenes among others. [17]
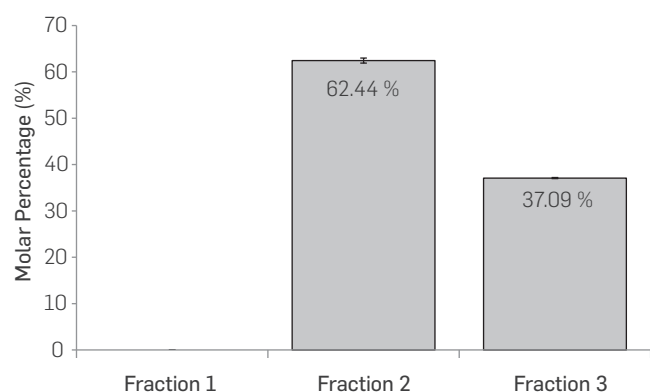
**Figure 1.** Molar percentage of each fraction of naphthenic acids in the commercial blend.

As previously stated, the corrosion tests were conducted using a *commercial blend of naphthenic acids* (MZ), as well as each of the fractions. As shown in Figure 2, the results confirm that fraction 1 is inert and did not cause any corrosion to the AISI SAE 1005 coupons. However, it was also observed that MZ has the lowest reactivity compared to fractions 2, 3 and 4, which suggests an inhibition effect by fraction 1 in the blend. Moreover, naphthenic acids included in fraction 2 were more reactive than those in fraction 3, which suggests that the fractionating method produces acids with different structural characteristics.
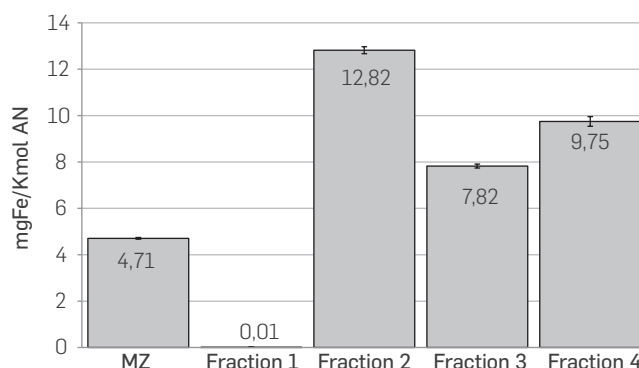
Figure 2. Reactivity of naphthenic acids on AISI SAE 1005, as a blend (MZ) and in the respective fractions, after 12 hours at 320°C.

CHARACTERIZATION OF FRACTIONS OF NAPHTHENIC ACIDS.

The FTIR-spectra of fractions 2 and 3 are shown in Figure 3. An intense band is observed at 1705 cm-1, which corresponds to the stretching of the C=O group in the carboxylic acids. In addition, a band between 2500 and 3500 cm-1was also observed, corresponding to tension vibration of the O-H group associated to the acidic function. The absorption due to off-plane bending of the OH bond results in
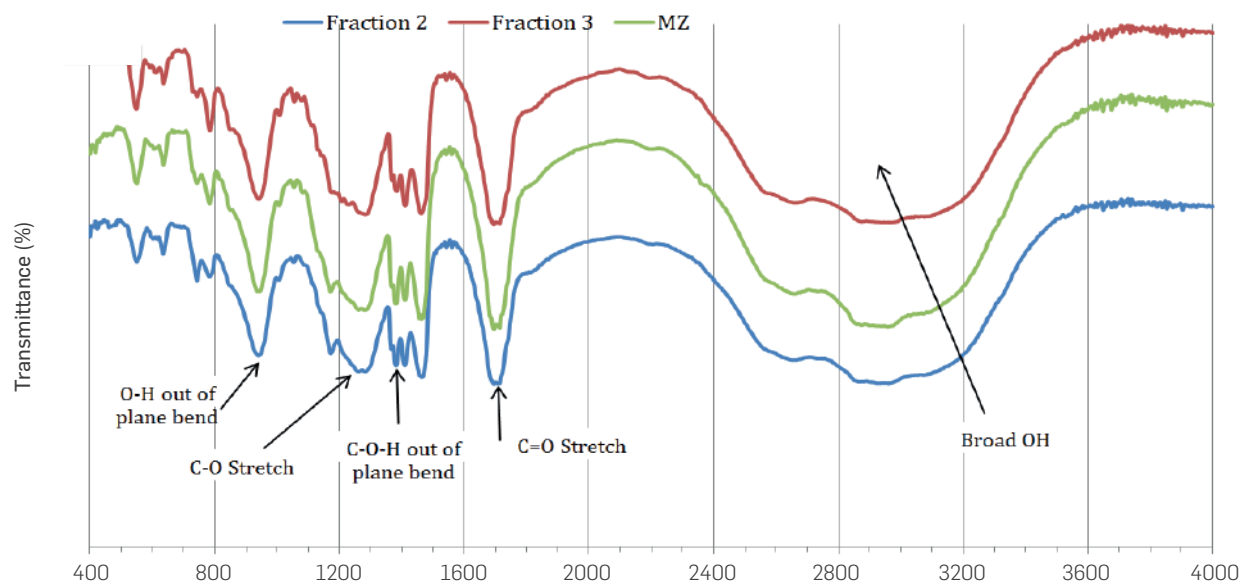
Figure 3. 3. FTIR-spectra of insoluble fractions 2 and 3.

the band observed at 930 cm-1. The asymmetric and symmetric stretching of the CH2 methylene groups was shown at 2924 and 2866 cm-1, respectively. The signal at 1377 cm-1 corresponds to off-plane bending of the C-O-H group, a characteristic of carboxylic acids. The signal corresponding to C-O bond stretching was observed at 1265 cm-1, while the vibrations of the methylene group appeared at 1378 and 1472 cm-1. The band corresponding to vibration balancing of the CH2 group at 720 cm-1 indicates the presence of this group in carbon chains of more than four carbons. The C=C absorption stretching in aromatic bonds was not observed between 1595 - 1620 cm-1. The spectra of the commercial blend and the respective fractions did not show significant differences with this method.

The average molecular weight of the fractions calculated by GPC and MS is included in Table 2. It shows that fraction 3 contains naphthenic acids of higher molecular weight compared to fraction 2. In general, a good match is observed in both analytical methods.

Table 2. Average molecular weight (Mw) of naphthenic acid fractions.

Fraction	M_W	
	GPC	MS
MZ	225.58	238.32
Fraction 2	290.05	300.12
Fraction 3	375.12	385.54
Fraction 4	305.25	295.01

The elemental composition of the fractions of naphthenic acids and the commercial blend is reported in Table 3. The results in Table 3 confirm that the C-to-H-ratio for fraction 3 is greater than for fraction 2, suggesting a lower degree of saturation in fraction 3. This is apparently associated with a greater amount of aliphatic chains or aromatic rings in fraction 2. Supposin that the remaining elemental composition can be attributed to oxygen, then MZ, fraction 2, fraction 3, and fraction 4 contain 13.64%, 11.63%, 9.11% and 7.38% of oxygen, respectively. Since each molecule contains one carboxyl group and no other forms of oxygen, a molecular formula can be calculated from the elemental analysis data. [15] Prototype naphthenic acids

have the following formulas and molecular masses: MZ: $C_{15.6} H_{23.2} O_2$ (M_W=241.93), fraction 2: $C_{17.7} H_{31.2} O_2$ (M_W = 275.14), fraction 3: $C_{23.5} H_{36.9} O_2$ (M_W = 351.15), and fraction 4: $C_{20.8} H_{34.2} O_2$ (M_W = 315.58). In fact, the calculated average molecular weights are close to those obtained experimentally by GPC and MS (Table 2).

Table 3. Elemental Analysis of the Commercial Mixture and the Fractions.

Elemental	MZ	Fraction 2	Fraction 3	Fraction 4
%C	76.75	77.04	80.37	79.01
%H	9.61	11.33	10.52	10.85
C/H	7.99	6.80	7.64	7.28

The complete assignment of the 1H NMR and 13C NMR spectrum, in terms of various hydrocarbon groups, is included in Table 4.

Structural parameters were determined from the 1H NMR spectra. The aromaticity of each test sample was calculated using Equation 17, where, A and B correspond to the integrals for the aromatic carbon band (from 100 to 170 ppm region), and the aliphatic carbon band (from 10 to 70 ppm region), respectively. A large number of equations for calculating the naphthenic ring number (R_N) have been reported. [18-20] However, in this case, the expression proposed by Molina et al. [21] included in Equation 18 was used. This expression has been used more frequently for the characterization of crude oil and derivatives.

$$fa = 100 \frac{A}{A+B} \tag{17}$$

$$R_N = \frac{C_{Nap} + C_{Ole}}{4.0} \tag{18}$$

C_{Nap} and C_{ole} are the naphthenic and olefinic carbon contents, respectively, determined with Equations 19 and 20:

$$C_{Nap} = [C9 - C9^0 - C9^1 - C9^2 - C9^3]C \tag{19}$$

$$C_{Ole} = H_4 H \tag{20}$$

Table 4. Assignment and Division of the ¹H NMR and ¹³C NMR Spectrum of naphthenic acid fractions for Measuring the Integral Intensity.

NMR	Regions		Structural Assignment
¹H NMR	0.5 – 2.0	$H_{\beta+\gamma}$	(β + γ) hydrogen band
	2.0 – 5.0	H_a	α hydrogen band
	11.0 – 12.0	H_{carb}	Carboxylic hydrogen bands
	0.5 – 12.0	H_T	Total hydrogen bands
	4.5 – 6.0	H_4	Olefinic Hydrogen
¹³C NMR	10.0 – 70.0	B	Aliphatic carbons
	100.0 – 170.0	A	Aromatic carbons
	21.5 – 50.0	C_g	Naphthenic and paraffinic carbons, CH2 y CH type.
	32.9	C_g^0	Methyne carbons (CH-CH3).
	23.0	C_g^1	Alpha methylene (CH2) to terminal methyl in alkyl chains.
	30.0	C_g^2	Methylenic carbons (CH2) in long chains, three and more carbons to final of chain.
	32.0	C_g^3	Methylenic carbon, third carbon atom from the end of chain or beta to aromatic rings.
	37.0	C_g^4	Methyne carbons to aromatic systems (CH2 bencilyc).

Equations 19 and 20 C and H contain the percentages of carbon and hydrogen for each sample (Table 4). Each alkyl side chain (n_{carbon}) *was defined as: (22)*

$$n_{carbon} = \frac{H_\alpha + H_\beta + H_\gamma}{H_\alpha} \qquad (21)$$

Where $H\alpha$, $H\beta$ and $H\gamma$ are equal to the integrals over α, β and γ hydrogen bands, respectively (Table 4). The percentage of hydrogen in carboxylic groups was determined from the following expression:

$$H_{carb}\,(\%) = 100\frac{H_{carb}}{H_T} \qquad (22)$$

Where H_{carb} and H_T can be determined by the integrals of the regions included in Table 4. Table 5 includes the structural parameters determined for the commercial mixture and the fractions.

Table 5. Structural Parameters of the Commercial Mixture and the Fractions.

| Parameter	MZ	Fraction 2	Fraction 3	Fraction 4
fa (%)	7.93	3.60	6.12	5.29
n_{carbon}	28.92	45.37	30.06	39.88
R_N	12.45	9.7	7.6	11.53
H_{carb} (%)	3.29	3.03	1.07	4.44

KINETIC STUDY

The kinetics of the corrosion reaction in the commercial blend and their respective fractions was adjusted to a second-order kinetics. The linear relationship between the inverse of the conversion (*X*) and the reaction time in the range of evaluated temperatures are shown in Figures 4 to 7 for the commercial blend, as well as for the different fractions

In addition, the kinetic constants for the corrosion reaction of the AISI SAE 1005 steel when exposed to the commercial blend as well as to the different fractions are presented in Table 6. The results confirm that the naphthenic acid corrosion reaction is an endothermic reaction in the temperature range evaluated in this study.
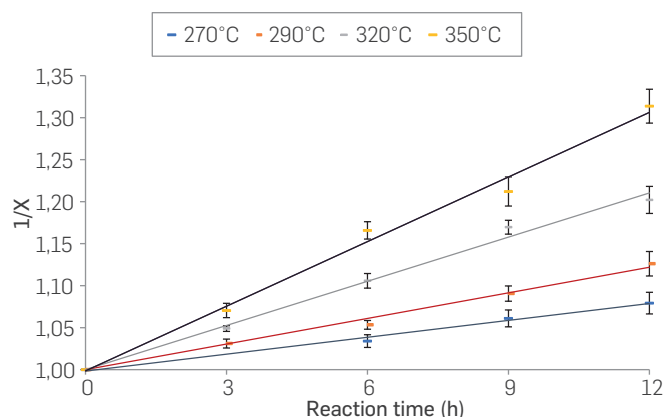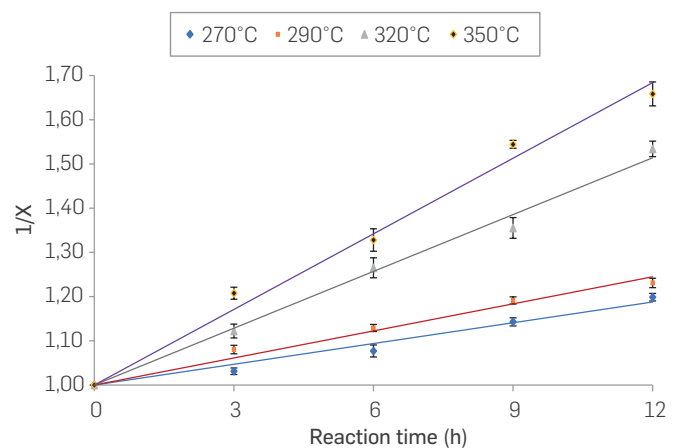

Figure 4. Corrosion kinetic plots for MZ at different temperatures.
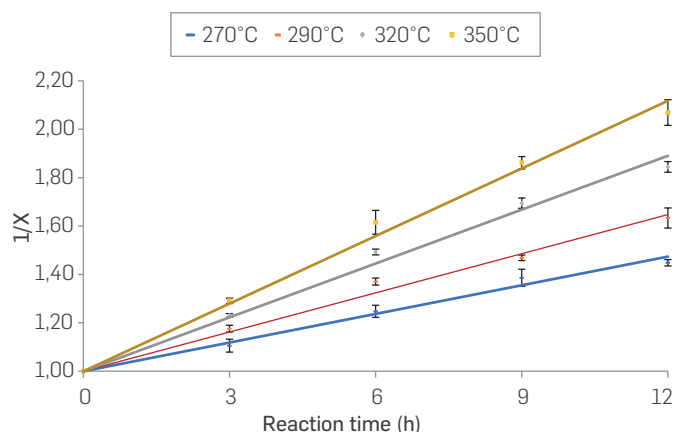
Figure 5. Corrosion kinetic plots for Fraction 2 at different temperatures.
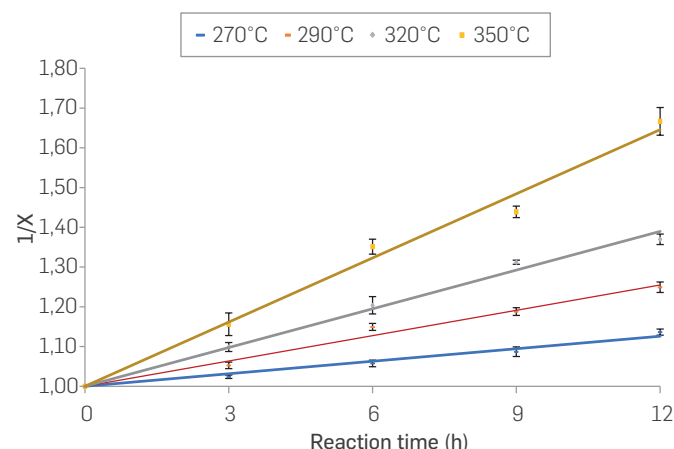
Figure 6. Corrosion kinetic plots for Fraction 3 at different temperatures.

Figure 7. Corrosion kinetic plots for Fraction 4 at different temperatures.

Naphthenic Acids Fractions	Reaction Rate Constant [g/mgKOH·h]							
	270°C		290°C		320°C		350°C	
	k	R^2	k	R^2	k	R^2	k	R^2
MZ	0.0008	99.09	0.0013	99.22	0.0023	99.20	0.0033	99.06
Fraction 2	0.0073	98.67	0.0100	98.83	0.0138	98.90	0.0173	99.16
Fraction 3	0.0016	98.36	0.0031	98.42	0.0048	99.05	0.0079	98.74
Fraction 4	0.0028	97.18	0.0037	97.91	0.0077	99.16	0.0102	98.85

Table 6. Reaction Rate Constant under Different Temperatures.

ARRHENIUS PLOT AND ACTIVATION ENERGY

The activation energy of the corrosion reaction driven by the naphthenic acids can be calculated from the linearization of the Arrhenius equation (Equation 23).

$$ln\ k = ln\ A - \frac{Ea}{RT} \tag{23}$$

Where k is constant reaction kinetics for each temperature, with units of g/mgKOH·h, A is the frecuency factor (g/mgKOHh), E_a is the activation energy (kJ/mol·K), R is the ideal gas constant (kJ/mol·K) and T corresponds to the absolute temperature (K). A and E_a can be calculated from the Arrhenius plot (Figure 8).
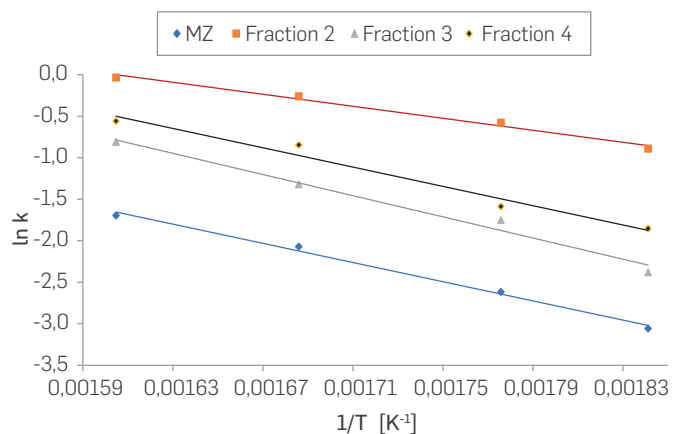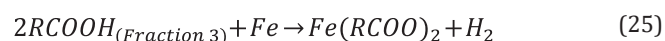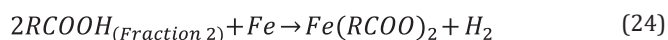

Figure 8. Arrhenius plots for the reaction between AISI SAE 1005 carbon steel and the commercial blend and the fractions.

Significant differences between the activation energy of Fraction 2 and Fraction 3 are observed in Figure 8, which are confirmed by the values included in Table 7. Apparently this difference relates to the structural characteristic of the naphthenic acids present in these fractions.

Table 7. Activation Energies from the Arrhenius Plots in Figure 8.

Naphthenic Acids Fractions	E_a (kJ/mol)	R^2
MZ	48.04	99.38
Fraction 2	29.90	98.78
Fraction 3	53.02	98.17
Fraction 4	48.31	97.42

Considering corrosion reactions of each fraction as parallel and independent.

$$2RCOOH_{(Fraction\ 2)} + Fe \rightarrow Fe(RCOO)_2 + H_2 \tag{24}$$

$$2RCOOH_{(Fraction\ 3)} + Fe \rightarrow Fe(RCOO)_2 + H_2 \tag{25}$$

The kinetic expression for each reaction is shown in equations 26 and 27.

$$-\frac{d\ [NA_2]}{dt} = k_{22} * [NA_2]^2 \tag{26}$$

$$-\frac{d\ [NA_3]}{dt} = k_{23} * [NA_3]^2 \tag{27}$$

Where $[NA_2]$ and $[NA_3]$ are the concentration of naphthenic acids of Fraction 2 and Fraction 3. k_{22}, k_{23} are the kinetic constants of the corrosion reaction of fraction 2 and fraction 3, respectively (Table 6). Integrating equations 26 and 27, the equations 28 and 29 were obtained. Equations 28 and 29 correspond to the naphthenic acid concentration in fraction 2 and fraction 3 at time t, respectively.

$$[NA_2]_{(t)} = \frac{1}{k_{22}t + \frac{1}{[NA_{2i}]}} \tag{28}$$

$$[NA_3]_{(t)} = \frac{1}{k_{23}t + \frac{1}{[NA_{3i}]}} \tag{29}$$

Then, the total moles reacting at time t corresponds to:

$$[NA]_{(t)} = [NA]i - [NA_2]_{(t)} - [NA_3]_{(t)} \tag{30}$$

Where $[NA]i$ is the initial concentration of naphthenic acids, while $[NA_2]_{(t)}$ and $[NA_2]_{(t)}$ correspond to the concentrations of naphthenic acids of Fraction 2 and Fraction 3 at time t. Given that in the corrosion reaction by naphthenic acids, two moles of naphthenic acids react with a mole of iron to produce iron naphthenate, then the concentration of iron dissolved in the solution at a time t, can be calculated from Equation 31:

$$[Fe]_{(t)} = \frac{[NA]_{(t)}}{2} \tag{31}$$

Substituting equation 30 in equation 31:

$$[Fe]_{(t)} = \frac{[NA]i - [NA_2]_{(t)} - [NA_3]_{(t)}}{2} \tag{32}$$

Substituting equations 28 and 29 in Equation 32:

$$[Fe]_{(t)} = \frac{[NA]i - \frac{1}{k_{22}t + \frac{1}{[NA_{2i}]}} - \frac{1}{k_{23}t + \frac{1}{[NA_{3i}]}}}{2} \tag{33}$$

The molar concentration of naphthenic acids can be determined using Equation 34:

$$[NA] = TAN \, W / 56000 \tag{34}$$

Where $[NA]$ is the concentration of naphthenic acids in mol/kg, TAN has been previously defined, and W corresponds to the mass (g) of the solution used in the reactor. The used units for the kinetic constants (Table 6) were changed to calculate the concentration of iron in solution using Equation 33. The obtained values are included in Table 8.

Table 8. Reaction Rate Constant for Fractions 2 and 3 at different Temperatures.

| Naphthenic Acids Fractions	Reaction Rate Constant kg/mol·h			
	270°C	290°C	320°C	350°C
Fraction 2	0.4107	0.5615	0.7715	0.9680
Fraction 3	0.0922	0.1737	0.2675	0.4428

The effect of the ratio of the molar fraction of naphthenic acids in fractions 2 and 3 on predicting the concentration of iron dissolved in mineral oil was also determined by using the values of the weight loss on AISI SAE 1005 carbon steel. The experimental conditions used for the validation tests are presented in Table 9.

**Table 9.** Parameters used in the Validation of the Kinetics Model

Parameter	Conditions
Temperature (°C)	270, 290, 320, 350
Reaction time (h)	12
$[NA_{2i}]/[NA_{3i}]$	0.18, 0.34, 0.46, 0.82, 1.00, 1.68, 2.50, 3.01, 3.50
TAN [mgKOH/g]	10
Material	AISI SE 1005

The correlation between the experimental and predicted values for the reactivity of the different molar ratios of fractions 2 and 3 as included in Table 9, is shown in Figure 9. In addition, the obtained %RMSE and EF values for the proposed kinetic equation to calculate the dissolution rate of iron due to naphthenic acid corrosion were 10.33% and 0.90, respectively. According to the statistical parameters, the kinetic model of parallel and independent reactions predicts appropriately the iron dissolution rate. The effect of the molar ratio of fractions 2 and 3 in the error percentage of the prediction model is shown in Figure 10. A significant increase in the prediction error is observed at the mid points of the molar ratio between fraction 2 and fraction 3, which can be explained by an interaction in the corrosion reactions related to each of these fractions.

A model that incorporates surface chemical reactions, solid state diffusion through growing corrosion product scales, and flow dynamics has been proposed by other researchers [23]. Such model has been validated using model molecules of naphthenic acids with good results in the prediction of the reaction kinetics. The incorporation of structural parameters of naphthenic acid mixtures, obtained in this investigation, will provide models with a better match to crude oil actual composition, complementing other proposed models.
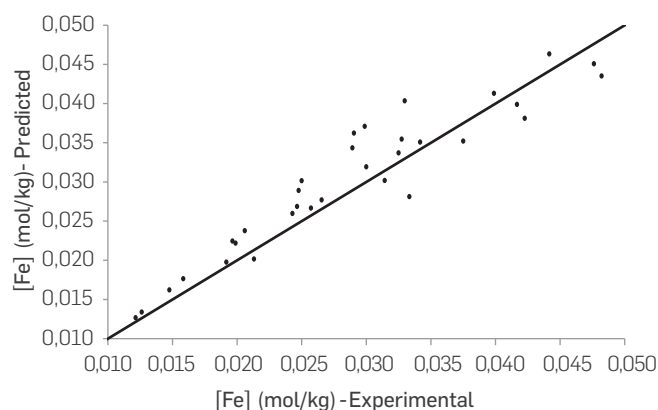
Figure 9. Validation of the proposed kinetic model for calculating the reactivity base on several molar ratios of fractions 2 and 3.
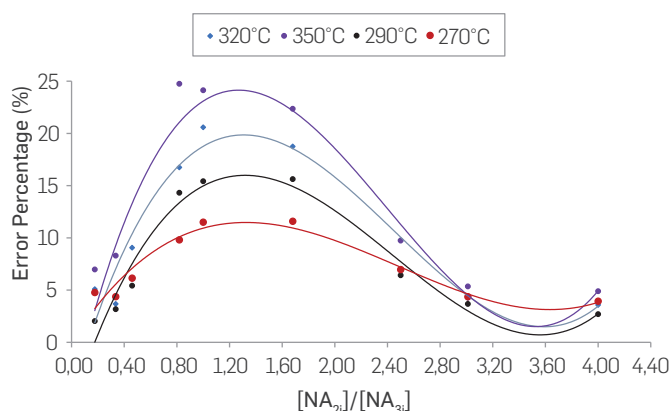
Figure 10. Effect of molar ratio $[NA_{2i}] / [NA_{3i}]$ on the error percentage of the proposed kinetic model for a reaction time of 12 hours.

CONCLUSIONS

This study successfully proposes and applies a methodology for conducting fractioning of a commercial blend into two fractions of naphthenic acids with different structural characteristics and chemical compositions.

Using the fractioning methodology introduced hereunder, two fractions with dissimilar reactivity, expressed as the amount of dissolved iron, were obtained from a commercial blend of naphthenic acids, and characterized by several analytical methods including FTIR, GPC, NMR and MS.

The particular elemental composition and structural parameters, added to the higher molecular weight determined for fraction 3, which has shown lower reactivity compared to fraction 2, suggest that it is formed with naphthenic acids with complex structures. Furthermore, it is considered that fraction 2 contains a larger amount of aliphatic chains or aromatic rings. In fact, the variation in the molar ratio of these two fractions seems to be the

reason for the differences in the corrosivity of crude oils having the same *TAN*.

██   A kinetic model using parallel and independent reactions is proposed for predicting the corrosivity of two fractions of naphthenic acids on AISI SAE 1005 carbon steel. The model reliably predicts the dissolution of iron in acidity ratios 2.4 < $TAN_{FRACTION2}$ / $TAN_{FRACTION3}$ <0.4. Outside this interval, the prediction error increases as a result of synergistic effects between the different fractions leading to the inhibition of the corrosion reaction.

REFERENCES

[1] Dettman, H.D., Li, N., Luo, J. (2009). Refinery corrosion organic acid structure, and Athabasca bitumen. Corrosion 2009, Nace International (ID 09336), Atlanta, USA

[2] Dettman, Heather; LUO, Jingli. (2010). The influence of naphthenic acid and sulphur compound structure on global crude corrosivity under vacuum distillation. CORROSION.

[3] Yepez, Omar (2007). On the chemical reaction between carboxylic acids and iron including the special case for naphthenic acid. *FUEL*, 86 (7-8), 1162-1168. https://doi.org/10.1016/j.fuel.2006.10.003

[4] Alvisi, P.P; Lins, Vanesa F.C. (2011) An overview of naphhthenic acid corrosion in a vacuum distillation plant. Engineering Failure Analysis, 18(5), 1403-1406, https://doi.org/10.1016/j.engfailanal.2011.03.019 .

[5] Qu, D.R, et al. (2006). High temperature naphthenic acid corrosion and sulphidic corrosion of Q235 and 5Cr1/2Mo steels in synthetic refining media. *Corrosion Science*, 48(8), 1960-1985. https://doi.org/10.1016/j.corsci.2005.08.016

[6] Biryukova, OV, et al. (2007). Biodegradation of naphthenic acids by rhizosphere microorganisms. *Chemosphere*, 67(10), 2058-2064. https://doi.org/10.1016/j.chemosphere.2006.11.063

[7] Saadine, T. (1996). *Review of critical factors affecting crude corrosivity*. CORROSION, (607).

[8] Mejía, C. Quiroga, H. Laverde, D. Hernandez, M and Gomez, M.A. (2012). A kinetic study of esterification of naphthenic acids from a Colombian heavy crude oil, *CT&F-Ciencia Tecnología y Futuro*, 4(5), 21-31. https://doi.org/10.29047/01225383.219

[9] Kapusta, D. (2004). *Safe processing of acid crudes*. CORROSION, 04637.

[10] Dettman, H. Li, N. and Luo, J. (2009). *Refinery Corrosion, organic acid structure and Athabasca bitumen*. CORROSION, 09336.

[11] Messer, B. Beaton, M. Tarlton, B. and Phillips. (2004). *New theory for naphthenic acid corrosivity of Athabasca Oil sands crudes*. CORROSION, 04634.

[12] Freitas, S., Malacarne, M.M., Romão, W., Dalmaschio, G.P., Castro, E.V.R., Celante, V.G., Freitas, M.B.J.G. (2013). Analysis of the heavy oil distillation cuts corrosion by electrospray ionization FT-ICR mass spectrometry, electrochemical impedance spectroscopy, and scanning electron microscopy. *FUEL*, 104, 656-663. https://doi.org/10.1016/j.fuel.2012.05.003

[13] ASTM International. (2012). ASTM G31-12a. *Standard Guide for Laboratory Immersion Corrosion Testing of Metals*, ASTM International, West Conshohocken, PA.

[14] ASTM International. (2007). ASTM D664-07, *Standard Test Method for Acid Number of Petroleum Products by Potentiometric Titration*, ASTM International, West Conshohocken, PA.

[15] Jego, G, etal. (2013). Calibration and performance evaluation of the STICS crop model for simulating timothy growth and nutritive value. *Field Crops Res.*, 151, 65-77. https://doi.org/10.1016/j.fcr.2013.07.003

[16] Jamieson, P.D, et al. (1991). A test of the computer simulation model ARCHWHEAI on wheat crops grown in New Zeland. *Field Crops Res.*, 27, 337-350. https://doi.org/10.1016/0378-4290(91)90040-3

[17] Muhammad, Khan, et al. (2016). A-non Catalytic supercritical methanol route for effective desacidification of naphthenic acids. *Fuel*, 182, 650-659. https://doi.org/10.1016/0378-4290(91)90040-3

[18] Rongbao, Li; ZENGMIN, Shen; BAILING, Li. (1988). Structural analysis of polycyclic aromatic hydrocarbons derived from petroleum and coal by 13C and 1H-n.m.r spectroscopy. *Fuel*, 67(4), 565-569. https://doi.org/10.1016/0016-2361(88)90355-9

[19] Williams, R.B. (1958). *Characterization of hydrocarbons in petroleum by nuclear magnetic resonance spectrometry*. Am. Test. Mater. Spec. Tech., 224, 168-194. https://doi.org/10.1520/STP46925S

[20] Quian, S.A, et al. (1985). Structural characterization of pitch feedstocks for coke making: use of 13C coupled 1H n.m.r. spectroscopy. *Fuel*, 64(8), 1085-1091. https://doi.org/10.1016/0016-2361(85)90111-5

[21] Poveda, Juan C, et al. (2012). Average molecular parameters of heavy crude oils and their fractions using NMR spectroscopy. *Journal of Petroleum Science and Engineering*, 84-85, 1-7. https://doi.org/10.1016/j.petrol.2012.01.005

[22] Wang, Xiaoqi; YONGAN, Gu. (2011). Characterization of Precipitated Asphaltenes and Deasphalted Oils of the Medium Crude Oil-CO2 and Medium Crude Oil-*n*-Pentane Systems. *Energy&Fuels*, 25(11), 5232-5241. https://doi.org/10.1021/ef201131n

[23] Jin, Peng; Robbins, W; Bota, G. (2018). Kinetic Reaction Modelling of Naphthenic Acid Corrosion and Sulfidation in Refineries – A Mechanistic Model. *CORROSION*, 74(12), 1351–1362. https://doi.org/10.5006/2880

AUTHORS

Carlos Mejía Miranda
Universidad Industrial de Santander, Grupo de Investigaciones en Corrosión. Bucaramanga, Colombia
ORCID: 0000-0001-6062-4032
e-mail: caumejia@gmail.com

Haydee Quiroga Becerra
Instituto Colombiano del Petróleo, ECOPETROL. Piedecuesta, Colombia.
ORCID: 0000-0002-9193-1438

Darío Yesid Peña Ballesteros
Universidad Industrial de Santander, Grupo de Investigaciones en Corrosión. Bucaramanga, Colombia
ORCID: 0000-0002-6193-9535

Dionisio Laverde Cataño
Universidad Industrial de Santander Grupo de Investigaciones en Corrosión. Bucaramanga, Colombia
ORCID: 0000-0002-1397-2429

Helmuth Sarmiento Klapper
Baker Hughes. Hannover, Alemania
ORCID: 0000-0001-5798-861X

Tecnologías diferenciadoras
PARA MITIGAR
el hurto de combustibles

- Contamos con una suite de tecnologías patentadas en cinco países que contribuyeron a reducir en **+95% las pérdidas por hurtos.**

- Capacidad diferenciadora para negociación con operadoras.

- Pérdidas por hurtos en el mundo superan los **USD$100 billones** por año (*).

* Por pérdidas y por inversiones en soluciones al problema.